A global forest canopy height map from the Moderate Resolution Imaging Spectroradiometer and the Geoscience Laser Altimeter System

Michael A. Lefsky[1]

Received 14 April 2010; revised 20 May 2010; accepted 1 June 2010; published 5 August 2010.

[1] The value of lidar derives from its ability to map ecosystem vertical structure which can be used to estimate aboveground carbon storage. Spaceborne lidar sensors collect data along transects and gain value for the global change science community when combined with data sources that have complete horizontal coverage. Data sources and methods for this type of analysis require evaluation. In this work we use image segmentation of 500 m Moderate Resolution Imaging Spectroradiometer (MODIS) data to produce a global map of 4.4 million forest patches. Where a Geoscience Laser Altimeter System (GLAS) transect intersects a patch, its height is calculated from the GLAS observations directly. Regression analysis is then used to estimate the heights of those patches without GLAS observations. Regression goodness-of-fit statistics indicate moderately strong relationships for predicting the 90th percentile patch height, with a mean RMSE of 5.9 m and mean correlation (R^2) of 0.67. **Citation:** Lefsky, M. A. (2010), A global forest canopy height map from the Moderate Resolution Imaging Spectroradiometer and the Geoscience Laser Altimeter System, *Geophys. Res. Lett.*, *37*, L15401, doi:10.1029/2010GL043622.

1. Introduction

[2] Improved global mapping of forest structure would provide critical information on the pools and fluxes of the global carbon cycle [*Drake et al.*, 2002] and mapping of biodiversity [*Turner et al.*, 2003] and the development of new technologies to map forest structure is a priority for international remote sensing agencies (NASA [*Dubayah et al.*, 2008], ESA [*Hese et al.*, 2005], *Japan Aerospace Exploration Agency* [2001]). New technologies are required because existing spaceborne methods cannot observe both the horizontal and vertical aspects of forest structure and biomass. Technologies based on passive optical sensing have shown limited sensitivity to forest structure above a low threshold of biomass [*Blackard et al.*, 2008], although they provide complete coverage in the horizontal plane. Microwave instruments, both polarimetric [*Waring et al.*, 1995] and inteferometric [*Treuhaft and Siqueira*, 2004], can map biomass over much of the earth's surface, but have difficulty where biomass is at its highest levels. Waveform lidar, another technology being evaluated for global mapping, is sensitive throughout the range of biomass [*Lefsky et al.*, 2005a, 2005b]. Each lidar waveform is a high spatial resolution record of the energy returned when a short-duration pulse of light is returned from the surface and interior of a forest canopy. For spaceborne sensors, however, lidar has incomplete horizontal coverage. Sensors planned for launch after the currently planned set of spaceborne missions still cover only a few percent of the earth's surface over a multiyear mission [*Zebker*, 2007]. All past and planned spaceborne lidar systems collect data in the form of transects of individual waveform observations spaced at some distance from each other. Until wide swath imaging lidar systems are available, these transect lidar data must be combined with optical or microwave images to extrapolate from individual lidar observations for complete horizontal coverage [*Dubayah et al.*, 2008].

[3] In this work we develop an approach to map forest height globally using lidar data from the Geoscience Laser Altimeter System (GLAS [*Abshire et al.*, 2005]) and multispectral data from the Moderate Resolution Imaging Spectroradiometer (MODIS). GLAS, onboard the Ice, Cloud, and land Elevation Satellite (ICESat), was a waveform sampling lidar sensor that emitted short duration (5 ns) laser pulses towards the land surface and recorded the echo of those pulses as they reflected off the ground surface. GLAS collected over 250 million waveform observations over forested areas globally during its 7 year mission, and its data can serve as a test bed for fusion of lidar data with imaging data that have complete horizontal coverage.

2. Methods

2.1. GLAS Data Processing

[4] GLAS data used for canopy height mapping were from cloud-free profiles acquired during observation periods L2A to L3I, which were conducted from September, 2003 to November, 2007. Data from period L2C were excluded from this sequence because the laser failed for a short time. After period L3I, laser power diminished to the point where we were no longer able to use the data. The GLAS sensor recorded waveforms, which have extents (distance from first to last energy) that are related to the height of the forest observed. The extent of these waveforms also increases with terrain slope, so the first step in GLAS data processing is slope correction [*Lefsky et al.*, 2005c, 2007]. The methods used here for terrain slope correction follow those of *Lefsky et al.* [2007], but the form of the equations is different and more stable when the extent of the waveforms leading and trailing edges are small.

[5] We used canopy height data from seven study areas to develop equations that estimate height from waveform extent indices. Five of the study areas have coincident

[1]Natural Resource Ecology Laboratory, Colorado State University, Fort Collins, Colorado, USA.

0094-8276/10/2010GL043622

GLAS waveforms and field estimates of height, and two of the study areas have coincident GLAS waveforms and estimates of height from airborne lidar remote sensing. Study areas with field height estimates are the Willamette Forest, (Oregon, USA), Great Smoky National Park (Tennessee, USA) and three study areas in the Brazilian Amazon (in the municipalities of Santarem, Para State; Manaus, Amazonas State; and Canarana, Mato Grosso State). Study areas with height estimates derived from discrete return lidar are the Tahoe National Forest (California, USA) and the Bartlett Experimental Forest (New Hampshire, USA). Sites, and plots within sites, were selected to bracket the range of terrain slope commonly associated with forests. Detailed descriptions of each study site and the sampling and lidar processing methods used for each are given by *Lefsky et al.* [2007].

[6] The index of height used in the processing of the global GLAS dataset is Lorey's height, the basal area weighted height of all trees. Basal area weighting of tree heights increases the importance of the largest trees in a stand and in general represents the height of the stand's tallest trees. Indices of total waveform extent and the height of the 10th and 90th percentile of waveform energy were used with least squares regression to estimate Lorey's height for the 484 plots in the seven focus study areas. An equation to estimate Lorey's height for broadleaf stands explained 83% of variance (R^2) with an RMSE of 3.3 m; for needleleaf stands the corresponding statistics were 79% and 4.9 m.

$$Lorey\_needle = 0.95 + (0.59*extent) - (0.106*lead10) - (0.074*trail10)(n = 389)$$

$$Lorey\_broad = -4.5 + (0.55*extent) - (0.102*lead10) - (0.0895*trail10)(n = 95)$$

For individual GLAS waveforms, physiognomy was determined by the MODIS land cover product (MOD12Q1). For waveforms associated with the "Mixed" physiognomy category, a third equation was used, which averaged the results of the other analyses. This equation explained 79% of variance in height with a 6.9 m RMSE.

$$Lorey\_mixed = -2.3 + (0.56*extent) - (0.106*lead10) - (0.0486*trail10)(n = 484)$$

Plots of predicted versus observed height for needleleaf and broadleaf stands are presented in Text S1 of the auxiliary material.[1]

2.2. Imagery

[7] Global coverage of monthly composited 7-band MODIS reflectance images at 500 m resolution for one year (2004) was retrieved from the Global Land Cover Facility. Global forest coverage was delineated into 50 5 × 5 degree subsets for processing. In each of these subsets, images were transformed using *Kauth and Thomas*'s [1976] approach [*Crist and Cicone*, 1984] to reduce data storage sizes while preserving most of the information content of the original images. This resulted in 12 images, each with 3 bands representing brightness, greenness, and wetness indices. Images for each of three indices for each month were layer stacked to create 3 images, each with 12 bands. These images were then PCA transformed, and the first three principal components were selected and layer stacked to create a single image with nine bands. The first three bands of the final image are the three brightness components, and so on for greenness and wetness.

2.3. Image Segmentation

[8] Individual GLAS waveform observations were collected every 172 m along north-south trending transects, commonly yielding two observations for each intersected pixel. More observations per pixel occasionally occur due to unusual geometry or more often due to multiple passes through the pixel. Given both the uncertainty of the GLAS-derived height measurement itself and the subpixel heterogeneity of the land surface, an estimate of height from two observations within a single 500 m pixel is likely to have high uncertainty. This issue is implicitly acknowledged in many remote sensing analyses that average multiple pixels together to create training data with lower uncertainty; these same studies commonly take analyses created using the spatially averaged data and apply them at the pixel level. To avoid this inconsistency, we use data averaged over patches as training data and also make height estimates using patches with the same size distribution as those used for the training data.

[9] To develop the patches used for training and height modeling, *Definiens* [2007] Developer 2007 was used to segment MODIS images into polygons based on their spectral and textural qualities. Definiens builds objects through a bottom-up procedure, starting from seed pixels and merging pixels (and then polygons) until user supplied spectral and spatial heterogeneity criteria are satisfied [*Benz et al.*, 2003]. These criteria can be spectral, in which case increases in heterogeneity are evaluated using pre- and post-merge spectral variability. They can also be spatial, in which case spatial heterogeneity is evaluated using smoothness, which is related to the ratio of the perimeter of the object to the area enclosing the object, and compactness, which is related to the ratio of the perimeter to the area within the polygon. In this work, spectral and spatial heterogeneity were considered to be equally important (scale parameter of 10.0, color/shape parameter set at 0.5, compactness parameter set at 0.0).

[10] After image segmentation, each polygon is attributed with the mean and standard deviation of each band and a suite of Haralick texture indices [*Haralick*, 1979] including grey level co-occurrence contrast, angular second moment, mean, standard deviation, and correlation. In addition, the polygons have attributes of modal MODIS land cover class, mean and standard deviation of the MODIS Vegetation Continuous Fields (Collection 4, Version 3 [*Hansen et al.*, 2003]) percent tree cover, and a biome class taken from the World Wildlife Federation's ecoregion classification [*Olson et al.*, 2001]. Each of these attributes is an independent variable used to model canopy height.

2.4. Canopy Height Modeling

[11] Two height statistics were calculated for each patch; the mean and 90th percentile of all GLAS estimates of height that fall in pixels classified as forest in the MODIS

[1] Auxiliary materials are available in the HTML. doi:10.1029/2010GL043622.

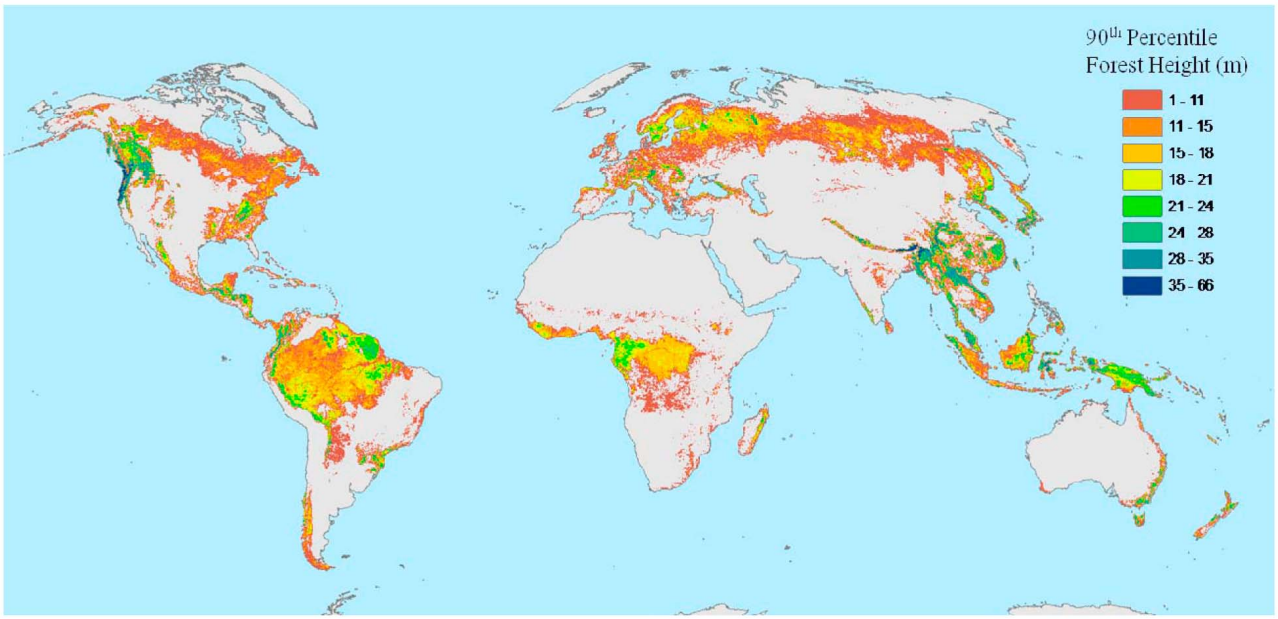

Figure 1. Global forest height map. Heights are the 90th percentile of GLAS height observations within a patch.

land cover product. Patches with intersecting GLAS transects were assigned these mean and 90th percentile height values directly. Patches without intersecting GLAS transects were assigned height values estimated using statistical modeling. There were 1,058,380 patches (23.9%) that had height observations within them and 3,375,635 that were modeled.

[12] Canopy height prediction equations for the patches without GLAS data were developed for each of 6 geographic regions (Australasia, Afrotropic, Indo-Malay, Nearctic, Neotropic, Palearctic, sensu *Olson et al.* [2001]) using Cubist (Rulequest-Research, Data mining with cubist, 2007, http://www.rulequest.com/cubist-info.html). Conventional regression approaches return a list of coefficients to be used with a specific equation to make estimates of a dependent variable. Cubist identifies multiple groups of observations that all have common relationships between independent and dependent variables and produces a list of rules that relate them. Each rule consists of a statement of the conditions it is valid for and an equation that estimates the dependent variable. Independent variables are used to define groups (condition variables) or linear equations that estimate the dependent variable for that group (model variables). Cubist was chosen because it creates equations than can be directly interpreted with respect to classes of response. Cubist was iterated twice; after the first pass, all points with a residual greater than 2 standard deviations were eliminated and Cubist was run a second time without the outlier points. The removal of these points is justified by the potential for true outliers due to land cover change, image quality, the uneven spatial distribution of GLAS observations, and the difficulty of examining each outlier separately. Datasets for model testing did not have these points removed. For the latter Cubist runs in each geographic region, a total of 48,872 polygons were randomly selected using stratification by height. These were separated into approximately equal sized training and test datasets by imposing a 25 km "checkerboard" grid on the globe and assigning patches to training or testing datasets on the basis of grid color.

3. Results

3.1. Image Segmentation

[13] The area of individual forested patches defined from MODIS image segmentation varies continuously from 25 ha (1 pixel) to over 225 km^2 (900 pixels), but the central distribution of patch sizes approximates a Gaussian distribution with a mean of 25 km^2 (100 pixels), a standard deviation of 50 km^2, and a right skew. Over 95% of patches were less than 64 km^2 or 256 pixels.

[14] Only patches with more than 200 GLAS observations were used for training and testing datasets. This number of observations was necessary to ensure that we had at least 1 observation per km^2.

[15] A map of median local patch size was created to allow comparison of algorithm performance globally. Developed areas have the smallest median patch size, whereas mountain chains have the largest. The northwest Amazon has large patches, while the north central Amazon has patches that are comparable in size to the suburbs of Sao Paulo. The intermountain west is the only area in the U.S. with moderate sizes, while most other areas have small median patch size.

3.2. Height Modeling

[16] For canopy height modeling with the Cubist statistical model, the average number of rules used in each of the 50 5 × 5 degree regions was 5 and the maximum was 13; all 32 independent variables were used in some Cubist rule. The five most important variables in the conditional statements were mean forest cover fraction, Brightness PC1, Greenness PC2, MODIS land cover, and the WWF biome code (49% of all used). Variables describing spectral means

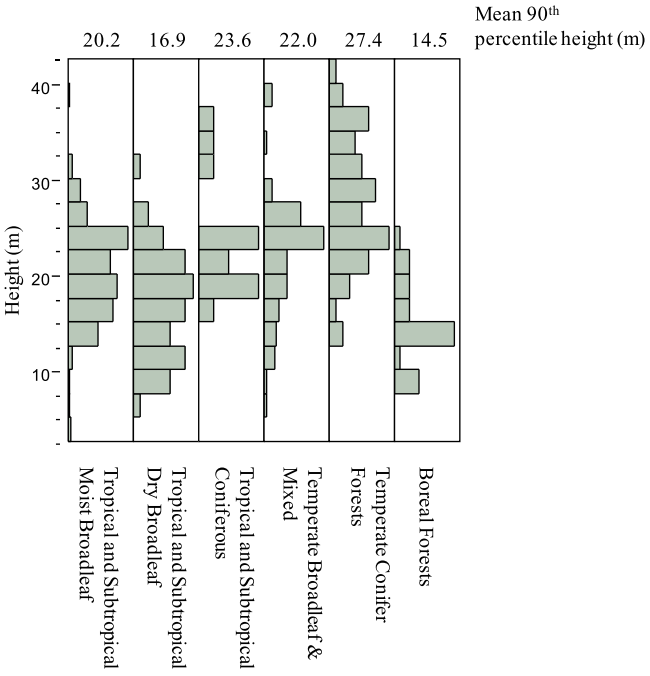

Figure 2. Distribution of heights for six broad forest classes.

within each patch (including principal components) accounted for 58% of the variables used in conditions, whereas those describing spectral variability (16%), Haralick texture indices (11%), and land cover and biome (13%) were less important. The three principle components of each spectral band made up nine of the ten most important variables used in the linear models. Brightness PC1, Wetness PC3 and Wetness PC2 were the three most important and were included in 25% of the rules. The types of variables picked to include in the linear equations were similar to the conditional variables, with variables describing spectral means making up 56% of the "model variables"; variability in the spectral bands (23%) and Haralick texture indices (20%) were less important.

[17] Goodness-of-fit statistics compiled for all for the training datasets in Cubist height modeling indicate moderately strong relationships. Estimates of 90th percentile height had RMSEs of 4.5 to 7, mean of 5.9, and correlations (R^2) of 0.56 to 0.77, mean of 0.67). Goodness-of-fit statistics for the test datasets were similar to those of the training dataset (mean RMSE 6.5 and mean r of 0.57) a sign that only slight over-fitting occurred. Full goodness of fit statistics for the 90th percentile and mean heights are included in Text S2. Figure 1 illustrates the 90th percentile height of the globe as calculated using this height modeling method, and Figure 2 reports the distribution of 90th percentile heights for each of the six forested classes.

4. Discussions

[18] This canopy height modeling procedure uses MODIS image segmentation as a tool to create patches as the basic spatial units representing land-surface conditions, the role conventionally filled by the individual pixel. If patches accurately represent variability in the landscape, then average spectral values for a patch should be as or more uniform than a square pixel of the same area. While the boundaries of the segmented patches seemed to follow natural features or the intersection of natural and anthropogenic features, there is no independent method for checking the degree to which image segmentation matches the landscape other than through additional image analysis.

[19] As expected, temperate conifer forests were the tallest, although patch-level averaging hid the very tallest stands. Boreal forests were shortest, and similar analysis indicates that among boreal forests, the deciduous boreal forests (i.e., larch) of north Asia are the shortest. The heights of tropical moist forests exceeded those of similar dry forests, but both were overtopped by tropical conifers and temperate broadleaf and mixed forests.

[20] There were only modest differences in height variability between the land cover classes. Temperate conifer forests had the highest variability, which reflects the range of these forest types, from pine barrens to stands of western hemlock. A regional breakdown shows that the Indomalay region has taller tropical and subtropical coniferous, temperate conifer and boreal forests than other regions, but shorter temperate broadleaf and mixed forests. The nearctic region has taller temperate conifer forests, and the afrotropic region has taller temperate broadleaf and mixed forests but shorter tropical and subtropical dry forests. The preceding statements are true at the $p < 0.05$ level based on simple ANOVA and t-tests.

[21] Moving to a patch based methodology has potential advantages. Rather than imposing an arbitrary geometric scale of land surface segmentation, the patch-based approach enables spatial segmentation based on canopy characteristics themselves, enabling the land cover characteristics to define appropriate analysis scale. With the use of patches, error could be quantified for individual landscape objects (e.g., forest stands), allowing us to define our uncertainty in the average conditions of both large and small patches. This approach provides a framework for developing a spatial hierarchy of information ranging from global and regional scales to more local scales. In a world of increased forest monitoring (e.g., for treaty compliance) a unified framework based on fitting multiple resolution data into a spatial hierarchy is a useful means of characterizing forest patterns for multiple purposes at multiple scales. Patch based segmentation provides us a hierarchy of management units to monitor while allowing reduced certainty when necessary.

[22] One implication of using patches is that, just as there is no one height that fully describes a tree, plot or stand, there is no one central tendency of height that describes a patch. In particular, with patches as large as those in this work, mean heights were consistently lower than we expected because they included disturbed areas within the patch at both the gap and larger scales, especially where forest and human habitation meet. As a consequence, it was necessary to have an index of height that captured the tallest heights in a stand; the 90th percentile height.

[23] In these analyses, 29.3% of patches had intersecting GLAS transects. While this provided a large training and testing data base (>1,000,000 patches), it is still limited by ICESat's mission requirement to repeat individual transects and by mission difficulties that led to a reduced sampling schedule. More GLAS observations, a randomly precessing orbit, and observations spread out over the satellite's

swath would allow much smaller patches and better spatial resolution. Full resolution images of the two canopy height maps can be downloaded at http://dl.dropbox.com/u/2104132/p_080809_global.img and http://dl.dropbox.com/u/2104132/x2_080809_global.img.

[24] **Acknowledgments.** This work was supported by NASA Terrestrial Ecology grants "Using the Geoscience Laser Altimeter System to Predict Forest Height & Biomass," "Spatially-Explicit Estimates of Forest Biomass in the Amazon Basin using MODIS and the Geoscience Laser Altimeter System" (NNG06GE11A), and NASA cryosphere grant "A Global Forest Canopy Height & Vertical Structure Product from the Geoscience Laser Altimeter System" (NNX06AH36G).

References

Abshire, J. B., X. Sun, H. Riris, J. M. Sirota, J. F. McGarry, S. Palm, D. Yi, and P. Liiva (2005), Geoscience Laser Altimeter System (GLAS) on the ICESat Mission: On-orbit measurement Performance, *Geophys. Res. Lett.*, *32*, L21S02, doi:10.1029/2005GL024028.

Benz, U. C., P. Hofmann, G. Willhauck, I. Lingenfelder, and M. Heynen (2003), Multi-resolution, object-oriented fuzzy analysis of remote sensing data for GIS-ready information, *ISPRS J. Photogramm. Remote Sens.*, *58*(3–4), 239–258.

Blackard, J. A., et al. (2008), Mapping U.S. forest biomass using nationwide forest inventory data and moderate resolution information, *Remote Sens. Environ.*, *112*, 1658–1677, doi:10.1016/j.rse.2007.08.021.

Crist, E. P., and R. C. Cicone (1984), A physically-based transformation of Thematic Mapper data—The TM tasseled cap, *IEEE Trans. Geosci. Remote Sens.*, *22*(3), 256–263, doi:10.1109/TGRS.1984.350619.

Definiens (2007), *Developer 7: User Guide*, Definiens Imaging GmbH, Munich, Germany.

Drake, J. B., R. O. Dubayah, R. G. Knox, D. B. Clark, and J. B. Blair (2002), Sensitivity of large-footprint lidar to canopy structure and biomass in a neotropical rainforest, *Remote Sens. Environ.*, *81*, 378–392, doi:10.1016/S0034-4257(02)00013-5.

Dubayah, R., et al. (2008), Global vegetation structure from NASA's DESDynI mission: An overview, *Eos Trans. AGU*, *89*(53), Fall Meet. Suppl., Abstract B31H-01.

Hansen, M. C., R. S. DeFries, J. R. G. Townshend, M. Carroll, C. Dimiceli, and R. A. Sohlberg (2003), Global percent tree cover at a spatial resolution of 500 meters: First results of the MODIS vegetation continuous fields algorithm, *Earth Interact.*, *7*(10), 1–15, doi:10.1175/1087-3562(2003)007<0001:GPTCAA>2.0.CO;2.

Haralick, R. M. (1979), Statistical and structural approaches to texture, *Proc. IEEE*, *67*(5), 786–804, doi:10.1109/PROC.1979.11328.

Hese, S., W. Lucht, C. Schmullius, M. Barnsley, R. Dubayah, D. Knorr, K. Neumann, T. Riedel, and K. Schrote (2005), Global biomass mapping for an improved understanding of the CO_2 balance—The Earth observation mission Carbon-3D, *Remote Sens. Environ.*, *94*, 94–104, doi:10.1016/j.rse.2004.09.006.

Japan Aerospace Exploration Agency (2001), Initiating the ALOS Kyoto and Carbon Initiative, in *Proceedings of the International Geoscience and Remote Sensing Symposium*, Inst. of Electr. and Electron. Eng., Sydney, N. S. W., Australia.

Kauth, R. J., and G. S. Thomas (1976), The tasseled Cap—A graphic description of the spectral-temporal development of agricultural crops as seen by LANDSAT, in *Proceedings of the Symposium on Machine Processing of Remotely Sensed Data*, pp. 41–51, Purdue Univ., West Lafayette, Indiana.

Lefsky, M. A., A. T. Hudak, W. B. Cohen, and S. A. Acker (2005a), Patterns of covariance between forest stand and canopy structure in the Pacific Northwest, *Remote Sens. Environ.*, *95*(4), 517–531, doi:10.1016/j.rse.2005.01.004.

Lefsky, M. A., A. T. Hudak, W. B. Cohen, and S. A. Acker (2005b), Geographic variability in lidar predictions of forest stand structure in the Pacific Northwest, *Remote Sens. Environ.*, *95*(4), 532–548, doi:10.1016/j.rse.2005.01.010.

Lefsky, M. A., D. J. Harding, M. Keller, W. B. Cohen, C. C. Carabajal, F. Del Bom Espirito-Santo, M. O. Hunter, and R. de Oliveira Jr. (2005c), Estimates of forest canopy height and aboveground biomass using ICESat, *Geophys. Res. Lett.*, *32*, L22S02, doi:10.1029/2005GL023971.

Lefsky, M. A., M. Keller, Y. Pang, P. de Camargo, and M. O. Hunter (2007), Revised method for forest canopy height estimation from the Geoscience Laser Altimeter System waveforms, *J. Appl. Remote Sens.*, *1*, 013537, doi:10.1117/1.2795724.

Olson, D. M., et al. (2001), Terrestrial ecoregions of the world: A new map of life on Earth, *BioScience*, *51*(11), 933–938, doi:10.1641/0006-3568(2001)051[0933:TEOTWA]2.0.CO;2.

Treuhaft, R. N., and P. R. Siqueira (2004), The calculated performance of forest structure and biomass estimates from interferometric radar, *Waves Random Media*, *14*(2), S345–S358, doi:10.1088/0959-7174/14/2/013.

Turner, W., S. Spector, N. Gardiner, M. Fladeland, E. Sterling, and M. Steininger (2003), Remote sensing for biodiversity science and conservation, *Trends Ecol. Evol.*, *18*(6), 306–314, doi:10.1016/S0169-5347(03)00070-3.

Waring, R. H., J. Way, E. R. Hunt, L. Morrissey, K. J. Ranson, J. F. Weishampel, R. Oren, and S. E. Franklin (1995), Imaging radar for ecosystem studies, *BioScience*, *45*, 715–723, doi:10.2307/1312677.

Zebker, H. (Ed.) (2007), DESDYNI report: Final report of the NASA Workshop, NASA, Orlando, Fla.

M. A. Lefsky, Natural Resource Ecology Laboratory, Colorado State University, 1472 Campus Delivery, Fort Collins, CO 80523, USA. (lefsky@cnr.colostate.edu)